

Supporting Information for:

**Solvent-induced structural transformation in luminescence
enhanced polymorphic Ionic HOFs**

Yi Yang, Bin Zhou, Yu-Ying Dai and Li-Hui Cao*

^aShaanxi Key Laboratory of Chemical Additives for Industry, College of
Chemistry and Chemical Engineering, Shaanxi University of Science and
Technology, Xi'an, 710021, P. R. China

E-mail:

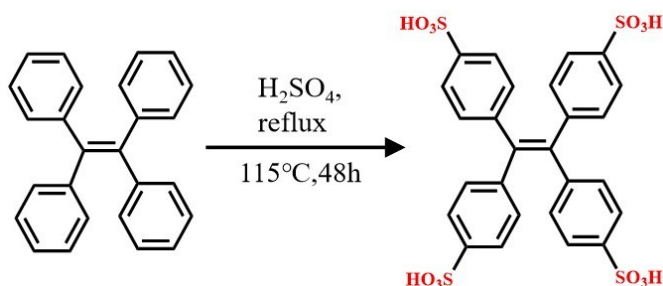
caolihui@sust.edu.cn

Section S1. Materials methods and experimental details

1.Materials and reagents: All reagents and solvents, including p-phenylenediamine, NaH, 4-Fluorobenzonitrile, *N, N*-Dimethylformamide (DMF), tetrahydrofuran (THF), lithium bis (trimethylsilyl) azanide (LiHMDS), ethanol (EtOH), hydrochloric acid (HCl), Tetraphenylethylene (TPE), concentrated sulfuric acid, ethyl acetate, methanol, *N, N*-Dimethylacetamide (DMA) and Dimethyl sulfoxide (DMSO) were obtained from commercial companies and used without further purification. Deionized water was used throughout all experiments wherever needed.

Synthesis of tetri (4-sulfonic phenyl) ethylene (H₄TPE):

H₄TPE was synthesised by a modified version of the reported method.



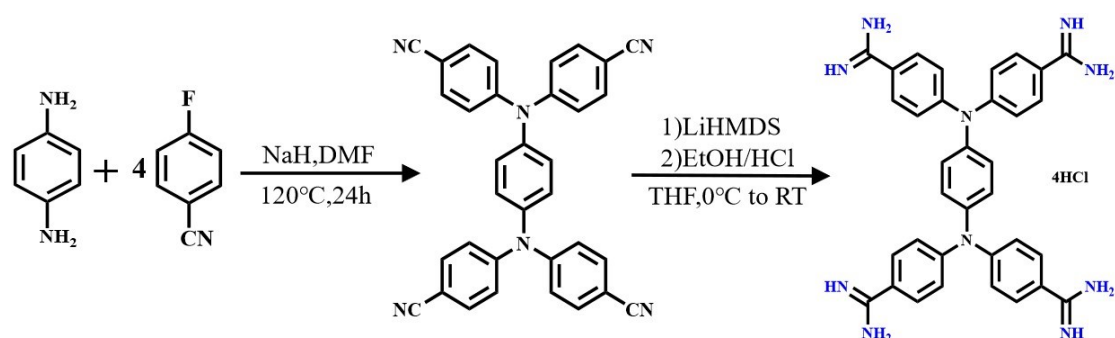
Scheme S1. Schematic representation of H₄TPE.

Add tetrathiophene (0.51 g, 1.5 mmol) to concentrated sulfuric acid (10 mL) heated to 115 °C. The solution was stirred at 115 °C for 4 hours. Add 30 mL of deionized water to the reaction mixture to quench the sulfuric acid and let the solution cool naturally. Then, slowly add the solution to ethyl acetate (at 0 °C). Filter the precipitated product and wash

the precipitate with 0 °C ethyl acetate three times. Dry the product at 80 °C to obtain 0.89 g of gray solid, yield: 90%¹.

Synthesis of 4,4',4'',4'''-(1,4-phenylenebis(azanetriyl)) tetrabenzimidamide (PATM):

The synthesis of PATM was accomplished with slight modifications based on the reported literature^{2,3}.



Scheme S2. Schematic representation of PATM.

1.92 g (80 mmol) of NaH was dissolved in 80 mL dry DMF. Stir at room temperature for about half an hour. Then add 2.16 g (20 mmol) of p-phenylenediamine and 11.60 g (96 mmol) of 4-Fluorobenzonitrile. In the presence of nitrogen protection, heat and stir the mixture at 120 °C for 24 hours, let it cool naturally to room temperature, and then precipitate with a mixture of 150 mL water and ethanol ($V_{\text{H}_2\text{O}}: V_{\text{EtOH}} = 1:1$). Filter the product and recrystallize it with ethanol to obtain a paleyellow solid of 8.20g, yield: 80%.

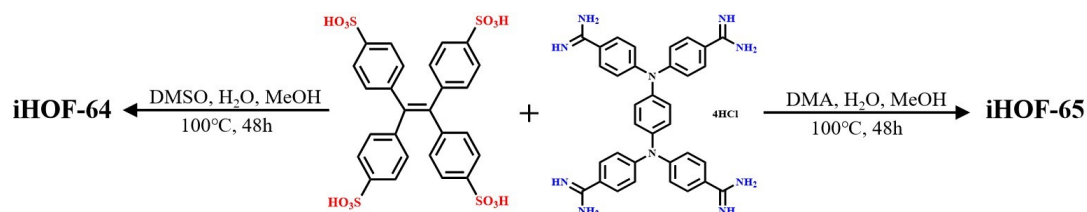
4,4',4'',4'''-(1,4-phenylenebis(azanetriyl)) tetrabenzonitrile (1.00 g, 1.95 mmol) was dissolved in dry THF (70 mL). The solution was cooled to -78 °C under N₂ atmosphere, and then LiHMDS solution (47 mL) was added immediately, resulting in the formation of a precipitate. The mixture was heated to room temperature and stirred for 10 hours. During this period, the precipitate dissolved to form a brown solution. The solution was cooled to 0 °C and then 3 mL acetyl chloride was added to 15 mL ethanol to prepare ethanol hydrochloride. A paleyellow precipitate was formed and ultrasonicated for 1 hour. After filtering out the solid, it was thoroughly washed with THF (100 mL) and then dried under vacuum, resulting in a yellow-brown powder-like PATM with a mass of 1.10 g, yield: 97%.

Synthesis of iHOF-64. H₄TPE (9 mg, 0.014 mmol) was completely dissolved in water (1 mL). At the same time, PATM (10 mg, 0.017 mmol) was dissolved in DMSO (1 mL). After ultrasonic dissolution, 1 mL of methanol was added. Then, the two clear solutions were mixed and loaded into the reaction vessel, which was placed in a 100 °C oven for 48 hours. The resulting product was a paleyellow transparent crystal.

Synthesis of iHOF-65. H₄TPE (8.6 mg, 0.013 mmol) was completely dissolved in water (1 mL). At the same time, PATM (7 mg, 0.0162 mmol) was dissolved in DMA (1 mL). After ultrasonic dissolution, 1 mL of methanol was added. Then, the two clear solutions were mixed and loaded

into the reaction vessel, which was placed in a 100 °C oven for 48 hours.

The resulting product was a paleyellow transparent crystal.



Scheme S3. Schematic representation for preparation of compound **iHOF-64/65**.

2.Characterization.

The powder X-ray diffraction (PXRD) measurement was carried out using a Cu X-ray source on the Bruker D8 Advance instrument, with the scanning range of $2\theta = 3.0 - 50.0^{\circ}$. The Fourier transform infrared spectroscopy (FT-IR) was obtained on the Bruker Vector-22 FTIR spectrometer, using potassium bromide sample sheets, and the wave number range was recorded from 4000 to 600 cm^{-1} . The ^1H NMR spectroscopy was recorded on the Quantum-I400MHz spectrometer, with the chemical shift expressed in ppm. The thermogravimetric analysis (TGA) measurement was conducted on the TGA-55 instrument, with the temperature ranging from room temperature to 800 °C, a heating rate of 10 °C/min, and in a nitrogen atmosphere. The solid-state UV-Vis spectroscopy was determined by the Cary 5000 spectrophotometer, and the fluorescence spectrum was recorded on the Edinburgh FLS-1000 fluorescence spectrometer (the test parameters of **iHOF-64/65** were kept consistent).

3. Single crystal X-ray diffraction.

The single-crystal X-ray diffraction data of compounds **iHOF-64** and **iHOF-65** were collected on a ROD, Synergy Custom DW system, HyPix diffractometer with Cu-K α radiation source ($\lambda=1.54184$ Å) at 100.00(10) K. All data were processed using the Olex2⁴ software, with the ShelXT⁵ structure solution program performing the internal phase method for structure solution, and the ShelXL⁶ refinement software package for least squares refinement. In the **iHOF-64** and **iHOF-65** structures, the H atoms connected to the main organic components and solvent molecules (water molecules and DMA molecules) were placed at the calculated positions and optimized using the riding model. For the severely disordered methanol solvent molecules, only the hydroxyl H atoms of the C61-O14 molecule with 0.784(9) occupancy in **iHOF-65** could be located from the difference-map plots and were included in the structural model with appropriate constraints. Satisfactory coordinates could not be determined for the H atoms of the remaining methanol sites. Therefore, these H atoms were not included in the structural model of **iHOF-64** and **iHOF-65**. For more details on the crystal data, please refer to the CIF files in the supporting crystallographic data. The complete structure solution data have been deposited in the Cambridge Crystallographic Data Centre, **iHOF-64** reference number CCDC 2501335 and **iHOF-65** reference number CCDC 2501334, and are available free of charge from CCDC.

Section S2. Ligand and Crystal Synthesis Characterization.

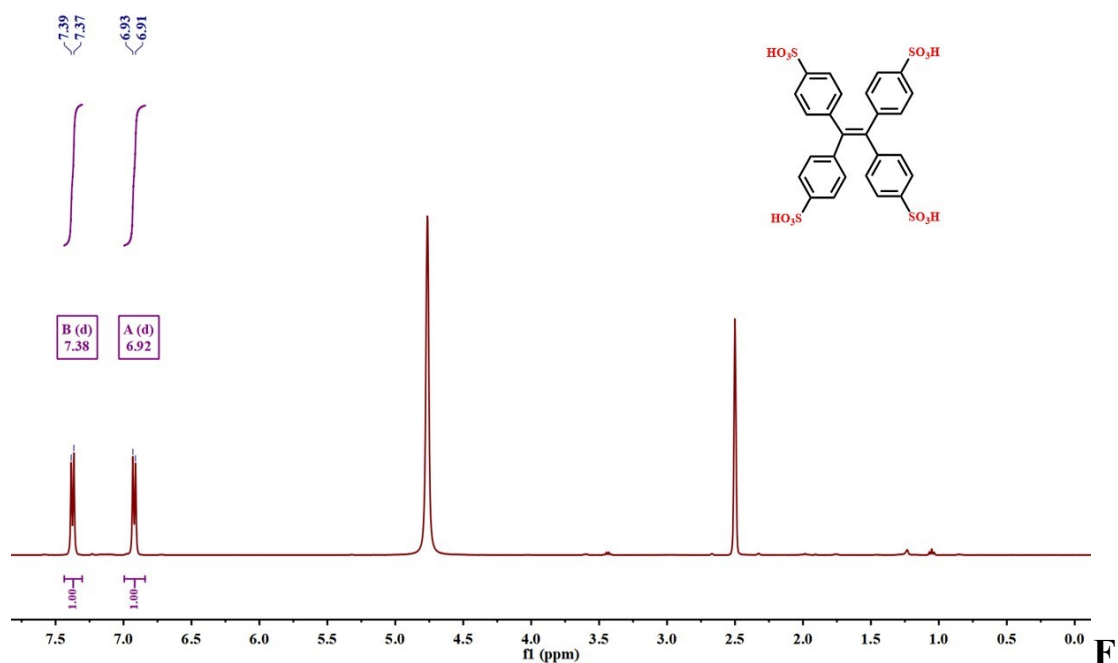


Figure S1. ¹H NMR spectrum of H₄TPE.

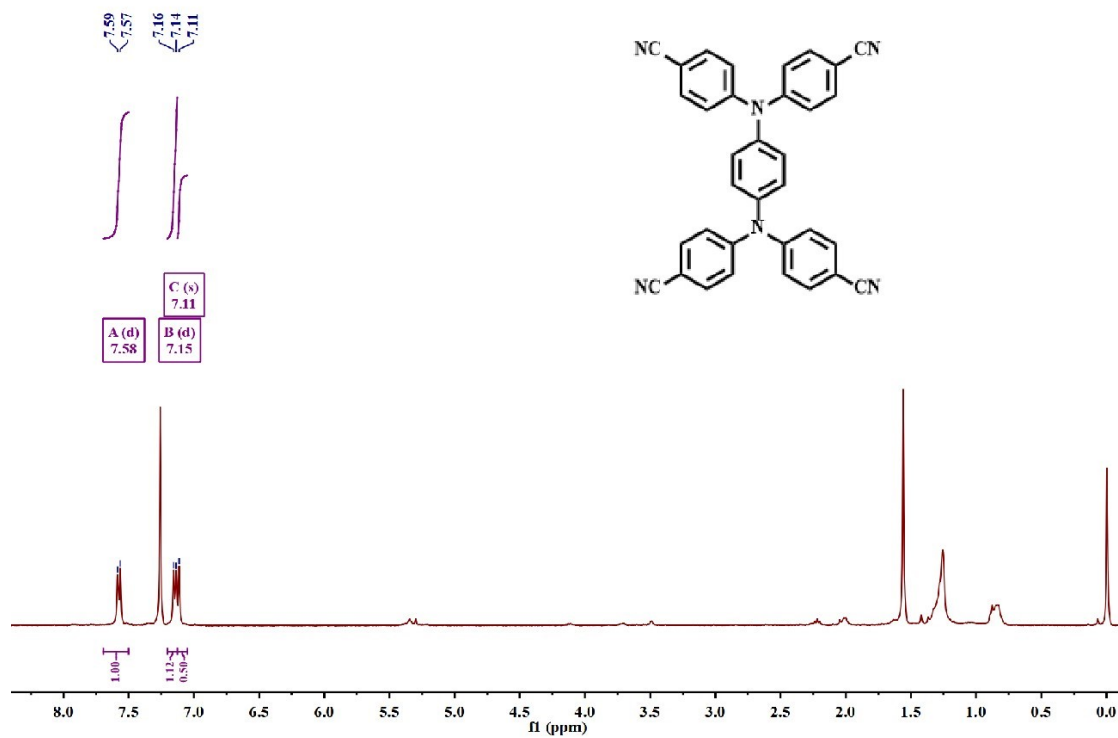


Figure S2. ¹H NMR spectrum of 4,4',4'',4'''-(1,4-phenylenebis(azanetriyl)) tetrabenzonitrile.

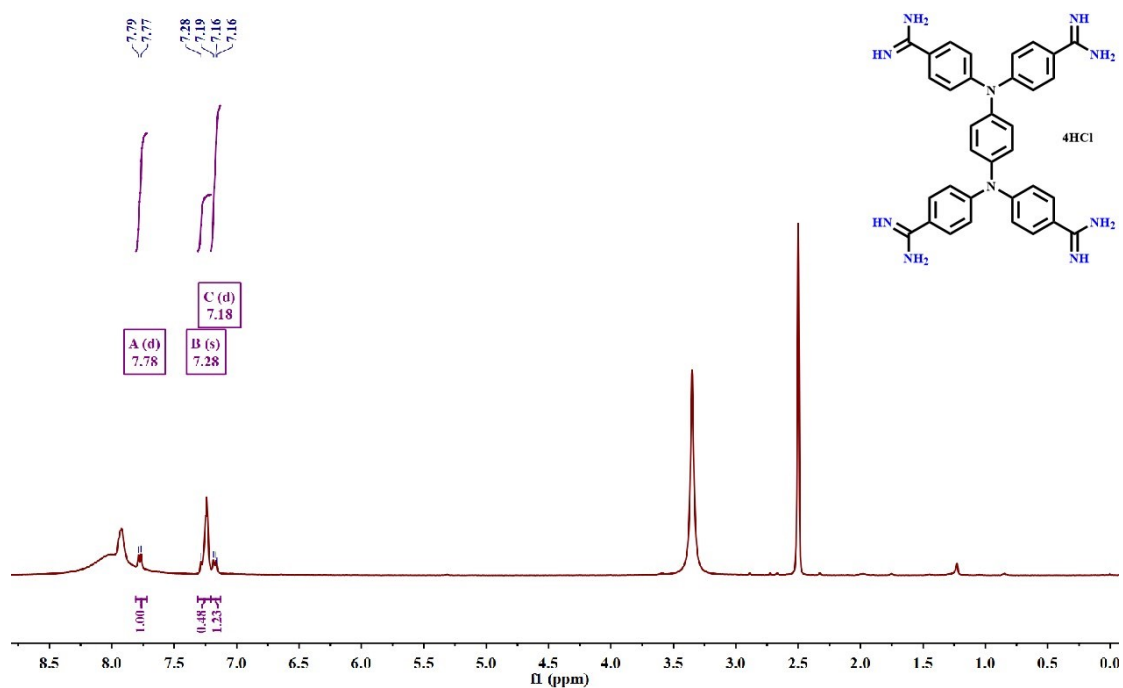


Figure S3. ¹H NMR spectrum of PATM.

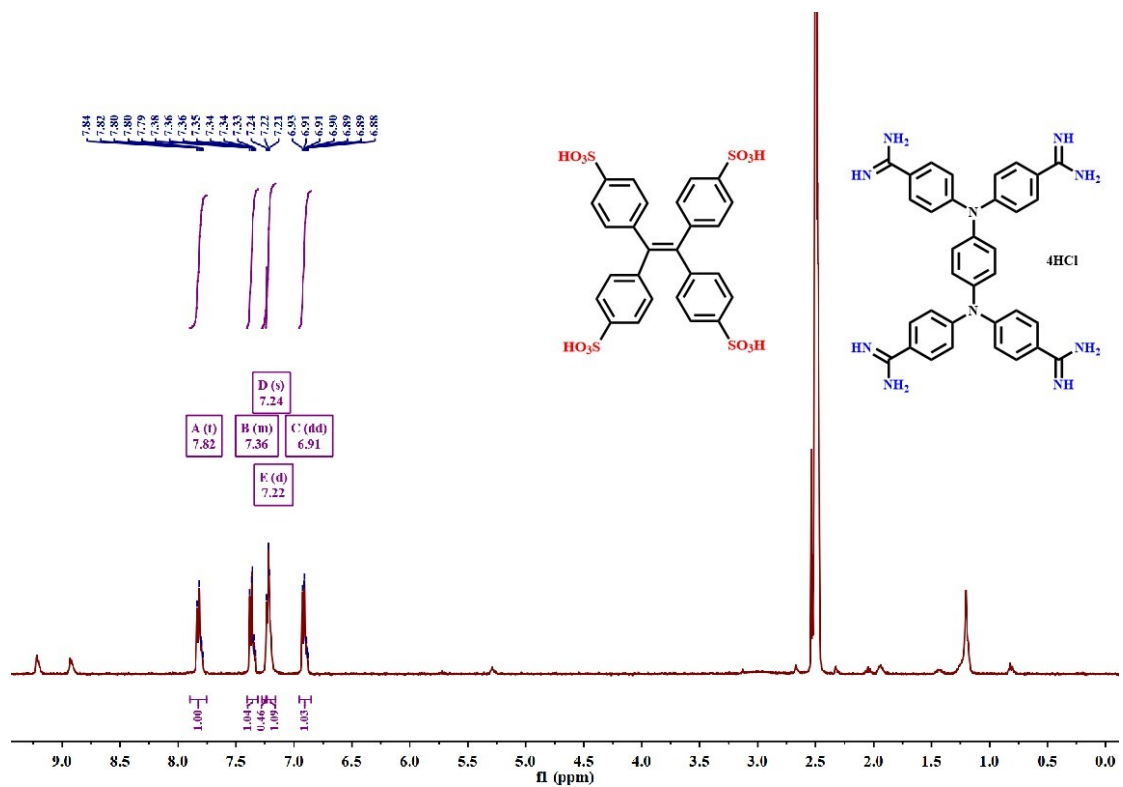


Figure S4. ¹H NMR spectrum of iHOF-64.

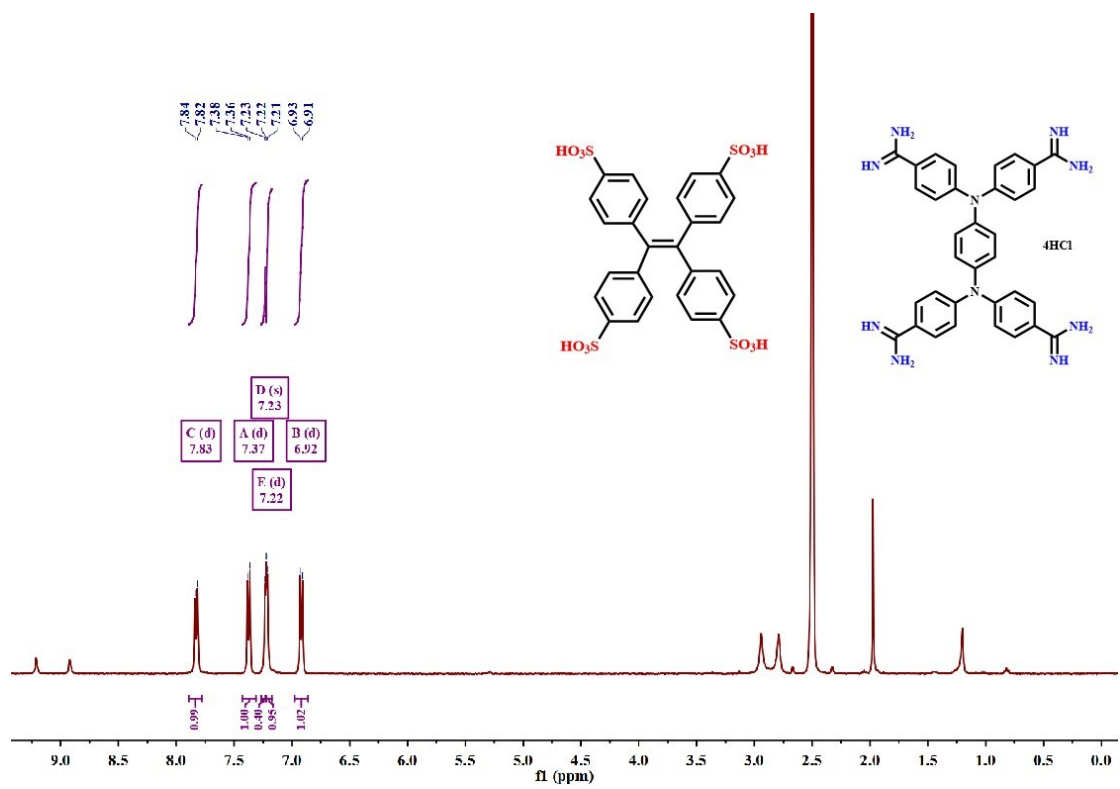


Figure S5. ^1H NMR spectrum of iHOF-65.

Section S3. Crystal Data and Structure.

Table S1. Crystal structure data and refinement details of **iHOF-64** and **iHOF-65**.

	iHOF-64	iHOF-65
Empirical formula	C ₁₃₁ H ₁₅₂ N ₂₀ O ₃₇ S ₈	C ₆₆ H ₇₁ N ₁₁ O ₁₆ S ₄
Formula weight	2855.20	1402.57
Temperature/K	100.00(10)	100.00(10)
Crystal system	triclinic	triclinic
Space group	<i>P</i> -1	<i>P</i> -1
<i>a</i> /Å	13.9046(2)	13.6618(3)
<i>b</i> /Å	14.5770(2)	14.7540(3)
<i>c</i> /Å	19.1732(3)	19.1796(5)
α /°	96.6140(10)	72.997(2)
β /°	111.196(2)	71.086(2)
γ /°	101.5510(10)	88.933(2)
Volume/Å ³	3474.23(10)	3484.95(15)
<i>Z</i>	1	2
ρ calc g/cm ³	1.365	1.337
μ /mm ⁻¹	1.910	1.872
<i>F</i> (000)	1502.0	1472.0
Radiation	Cu K α (λ = 1.54184)	Cu K α (λ = 1.54184)
2 θ range for data collection/°	5.052 to 151.598	5.11 to 152.138
Index ranges	-17 ≤ <i>h</i> ≤ 17, -18 ≤ <i>k</i> ≤ 18, -20 ≤ <i>l</i> ≤ 24	-17 ≤ <i>h</i> ≤ 11, -18 ≤ <i>k</i> ≤ 18, -24 ≤ <i>l</i> ≤ 21
Reflections collected	43221	38633
Independent reflections	14122 [R _{int} = 0.0434, R _{sigma} = 0.0440]	14092 [R _{int} = 0.1040, R _{sigma} = 0.0720]
Data/restraints/parameters	14122/763/1098	14092/453/1027
Goodness-of-fit on F ²	1.048	1.050
Final R indexes [I ≥ 2 σ (I)]	R ₁ = 0.0570, wR ₂ = 0.1611	R ₁ = 0.0985, wR ₂ = 0.2522
Final R indexes [all data]	R ₁ = 0.0671, wR ₂ = 0.1690	R ₁ = 0.1131, wR ₂ = 0.2629
Largest diff. peak and hole/e. Å ⁻³	0.64/-0.60	0.99/-0.78
CCDC number	2501335	2501334

$${}^a R_1 = \sum ||F_o| - |F_c|| / \sum |F_o|, {}^b wR_2 = \{ \sum [w(F_o^2 - F_c^2)^2] / \sum [w(F_o^2)^2] \}^{1/2}$$

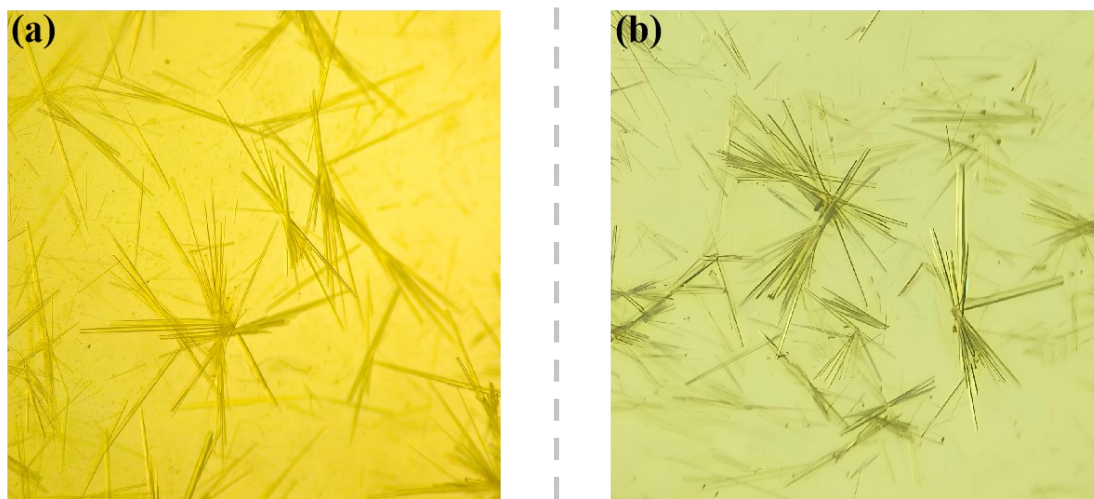


Figure S6. (a) iHOF-64 and (b) iHOF-65 crystals photograph.

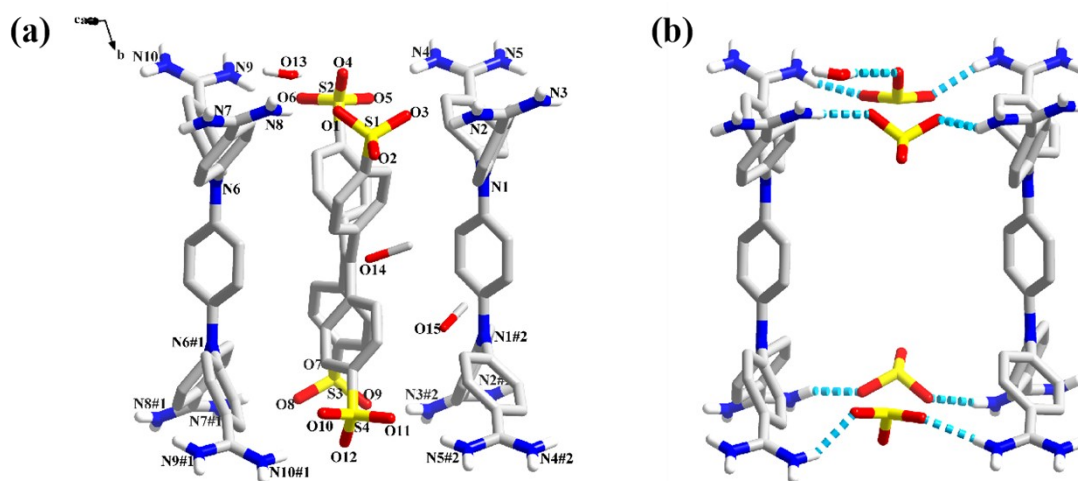


Figure S7. (a) The asymmetric unit of iHOF-64. Symmetry codes: #1: $2-x, 1-y, 2-z$; #2: $1-x, 1-y, 1-z$. (b) Hydrogen-bonded connection mode of sulfonate anion and guanidinium cation.

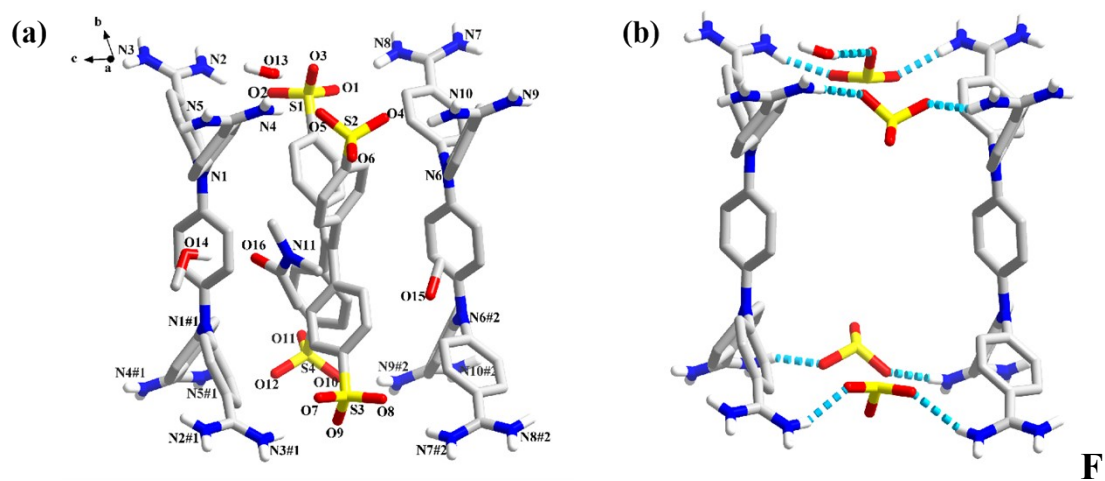


Figure S8. (a) The asymmetric unit of **iHOF-65**. Symmetry codes: #1: 1-x, 1-y, 1-z; #2: 1-x, 1-y, -z. (b) Hydrogen-bonded connection mode of sulfonate anion and guanidinium cation.

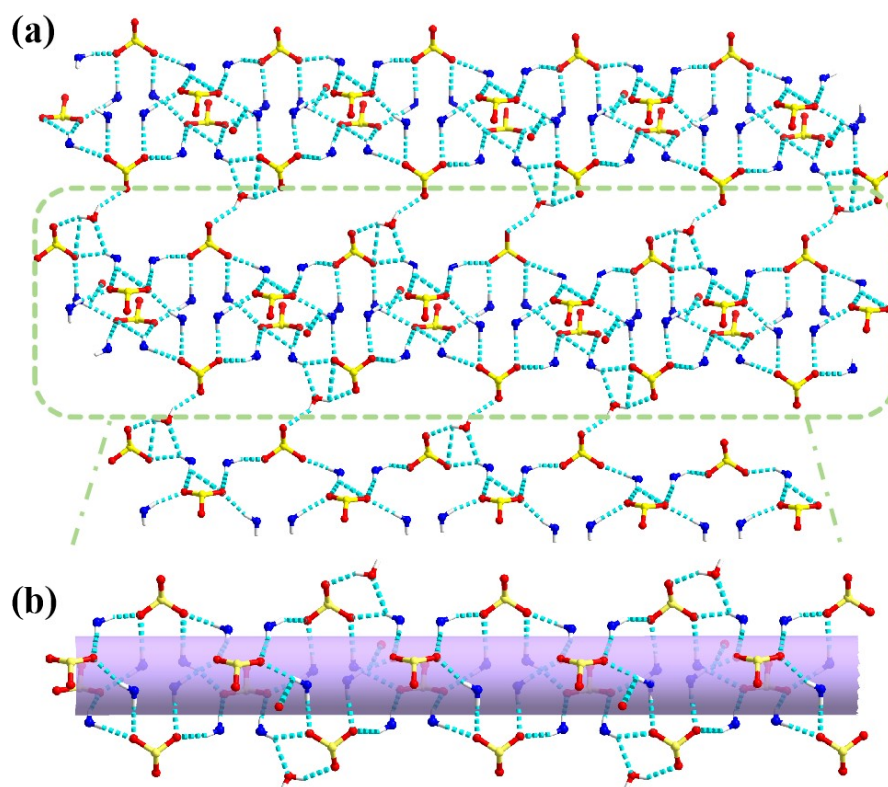


Figure S9. (a) 2D hydrogen-bonded network and (b) small hydrogen-bonded channels in **iHOF-64** supramolecular structure.

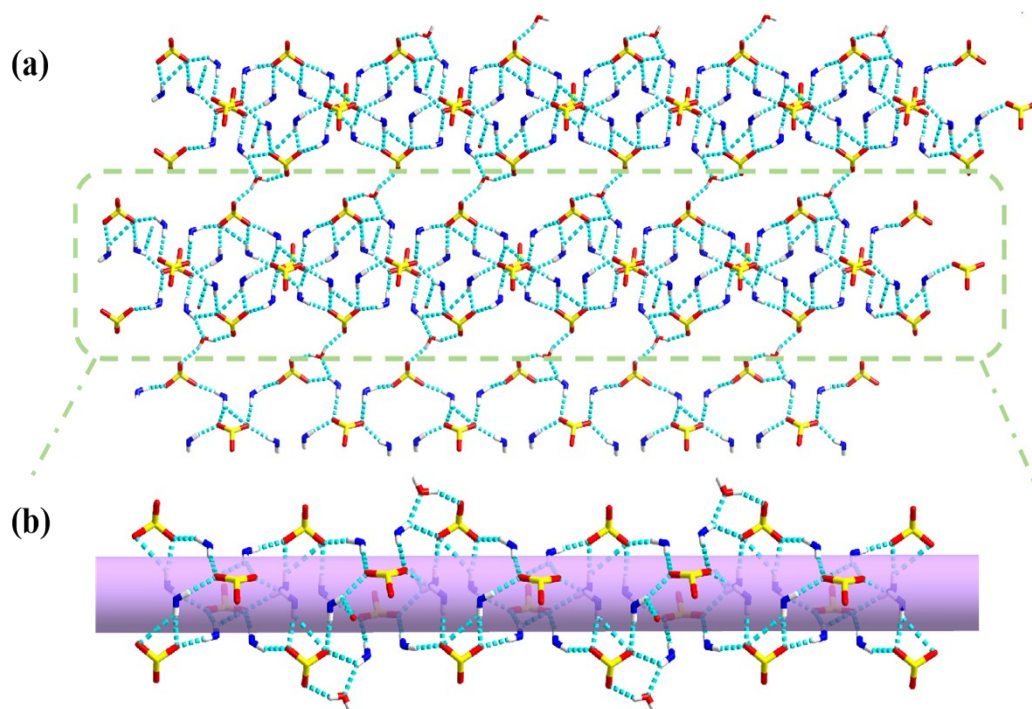


Figure S10. (a) 2D hydrogen-bonded network and (b) small hydrogen-bonded channels in **iHOF-65** supramolecular structure.

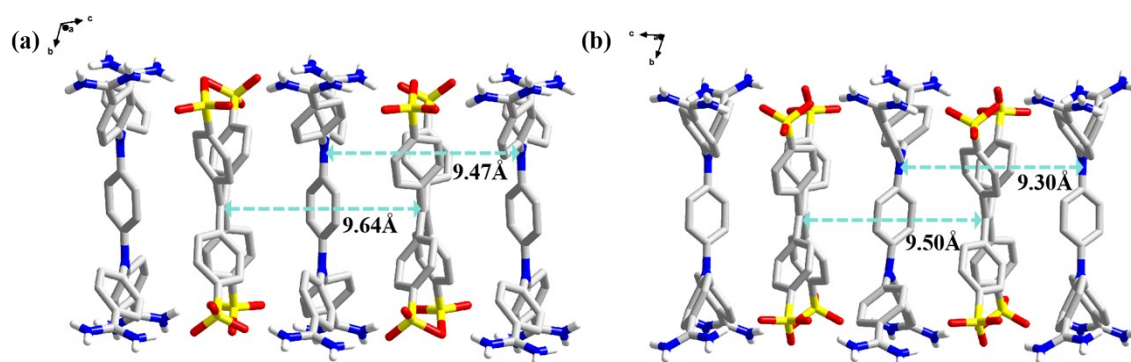


Figure S11. The distance between H₄TPE and PATM in the structures of (a) **iHOF-64** and (b) **iHOF-65**.

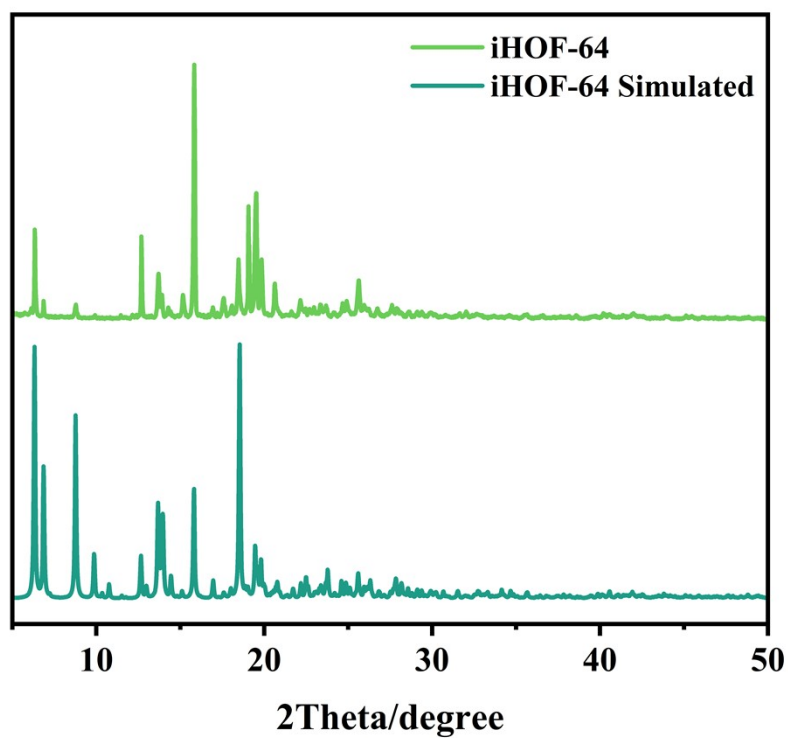


Figure S12. PXR D patterns of iHOF-64.

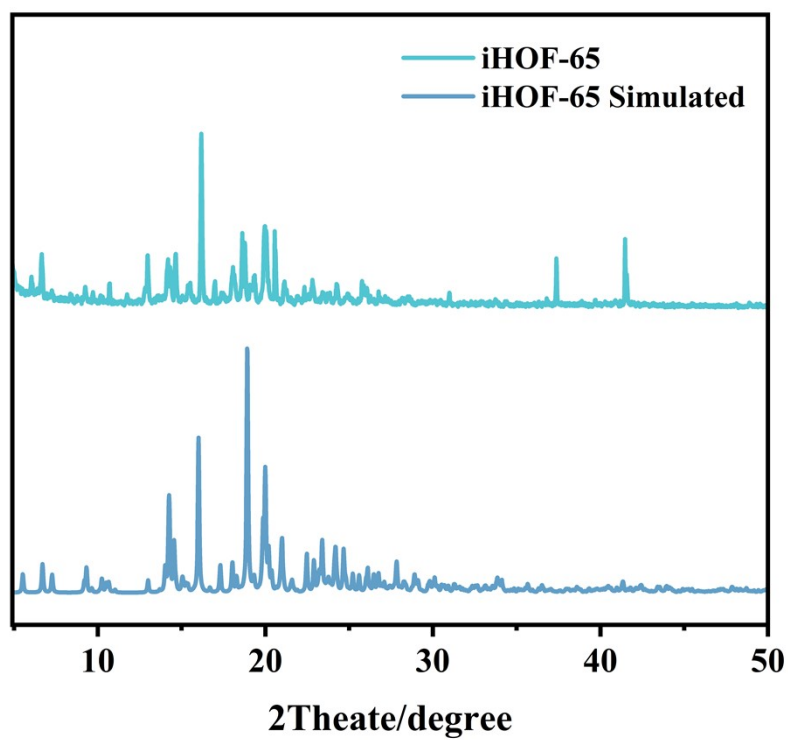


Figure S13. PXR D patterns of iHOF-65.

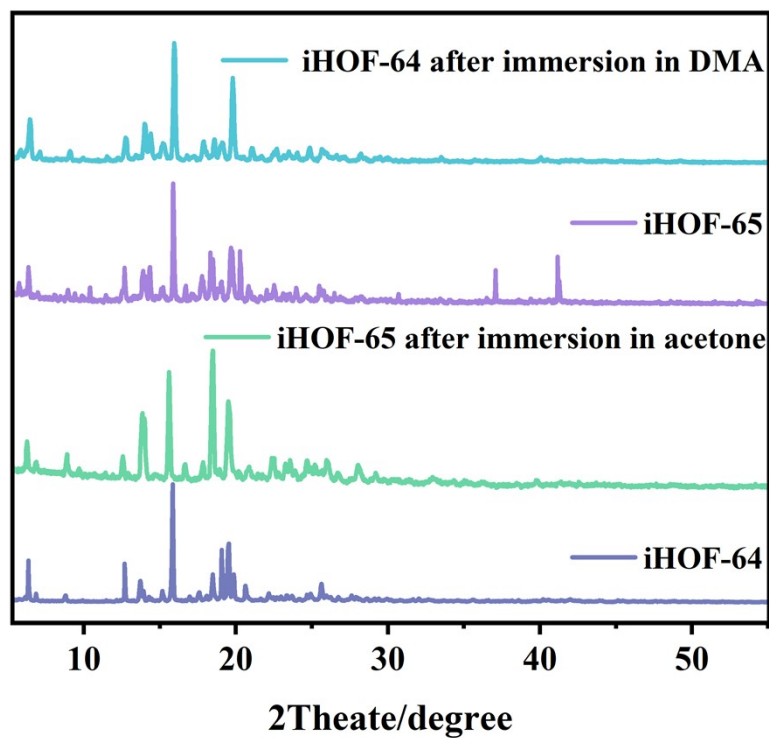


Figure S14. The PXR D patterns of the conversions of **iHOF-64** and **iHOF-65**.

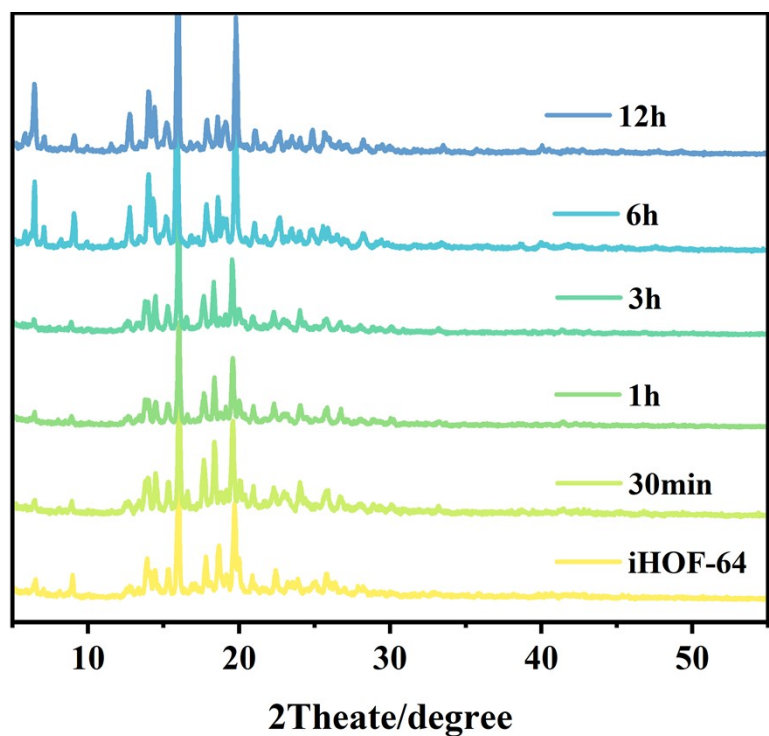


Figure S15. The PXR D patterns of **iHOF-64** after being immersed in DMA solvent for different times.

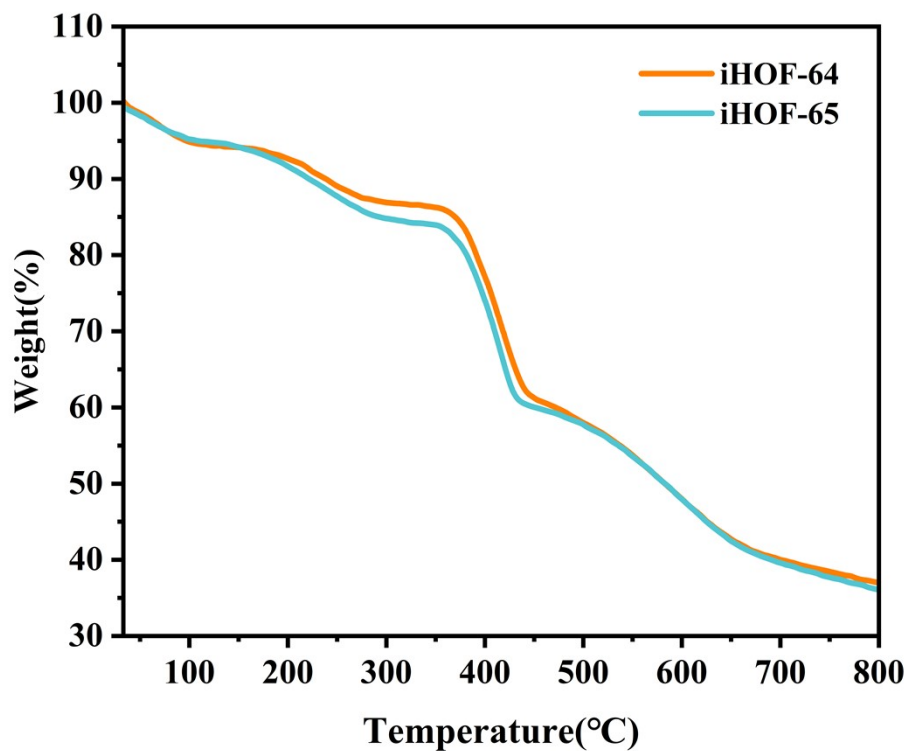


Figure S16. TGA plots of iHOF-64 and iHOF-65.

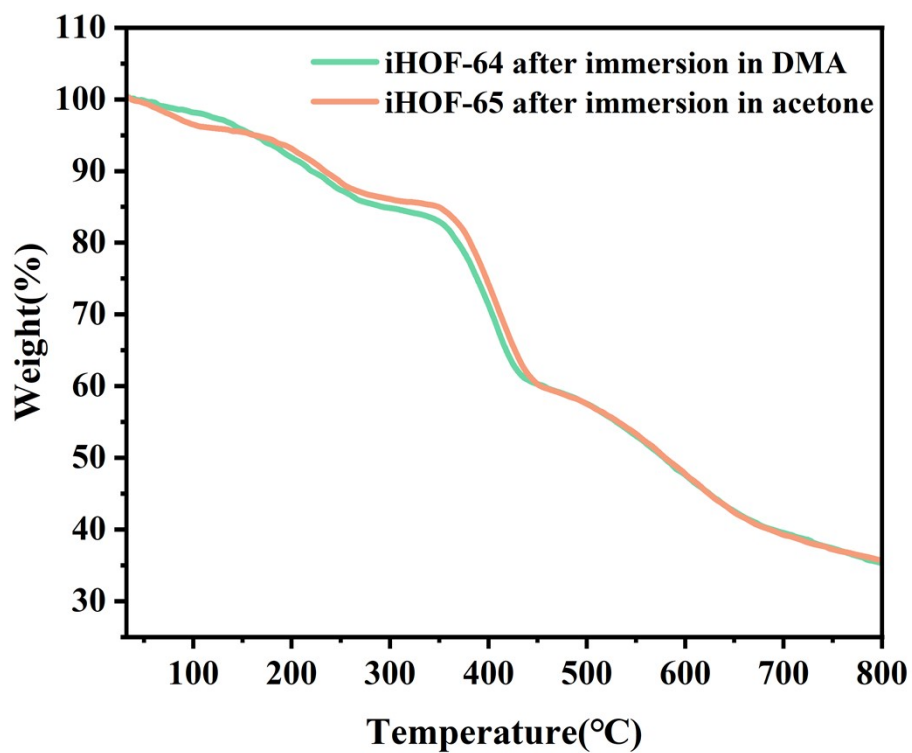


Figure S17. TGA plots of the structurally transformed iHOF-64 and iHOF-65.

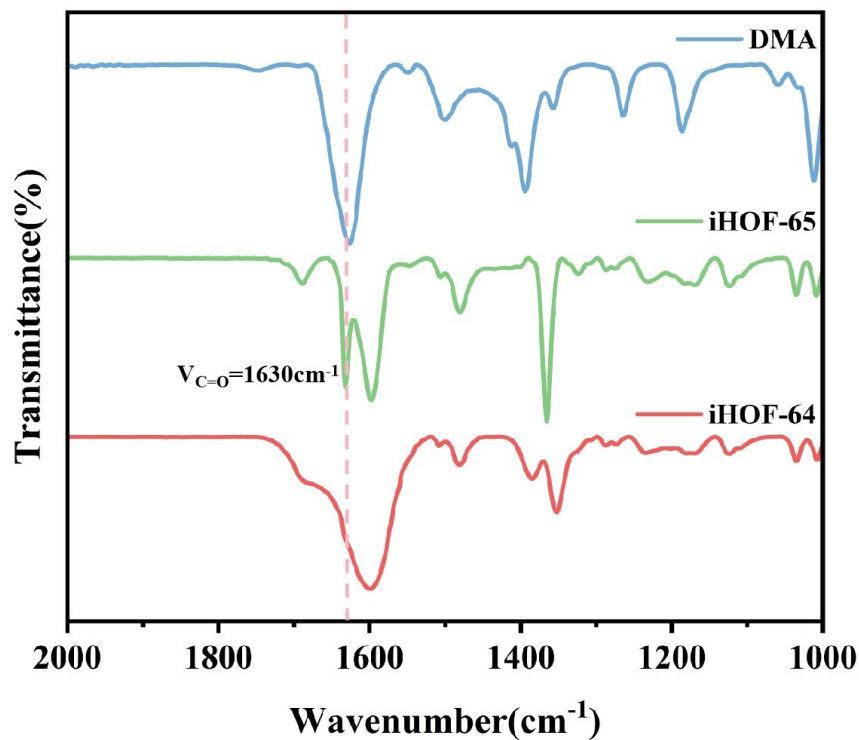


Figure S18. FT-IR of iHOF-64, iHOF-65 and DMA.

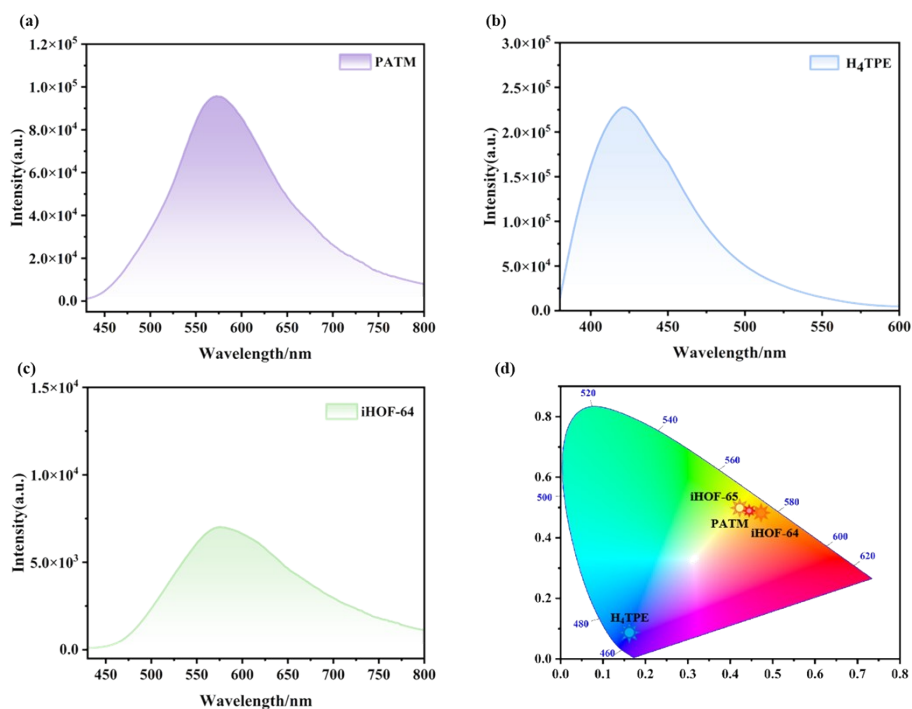


Figure S19. (a) The fluorescence emission spectrum of PATM ($\lambda_{\text{ex}}=400$ nm).

(b) The fluorescence emission spectrum of H₄TPE ($\lambda_{\text{ex}}=360$ nm). (c) The

fluorescence emission spectrum of **iHOF-64** ($\lambda_{\text{ex}}=365$ nm). (d) The CIE diagrams of PATM, H₄TPE, **iHOF-64** and **iHOF-65**.

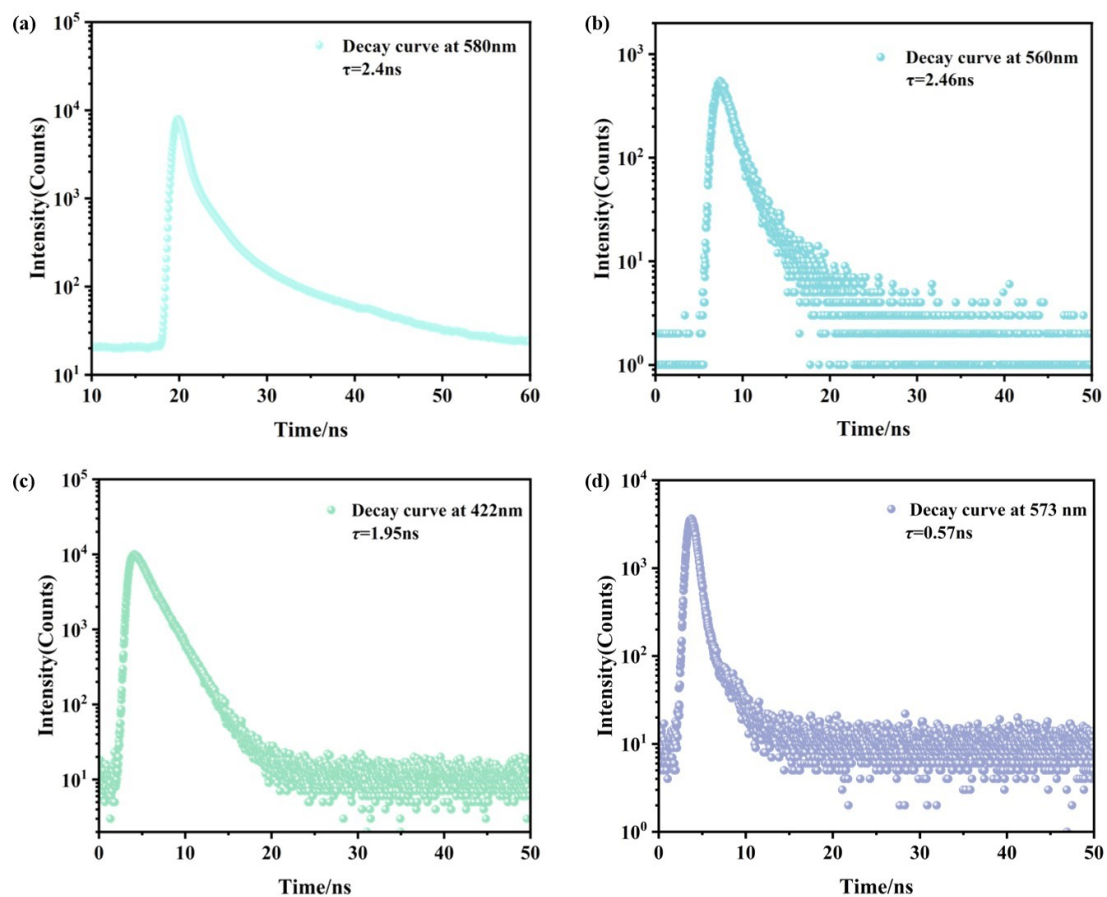


Figure S20. (a) The fluorescence lifetimes of **iHOF-64**. (b) The fluorescence lifetimes of **iHOF-65**. (c) The fluorescence lifetimes of H₄TPE. (d) The fluorescence lifetimes of PATM.

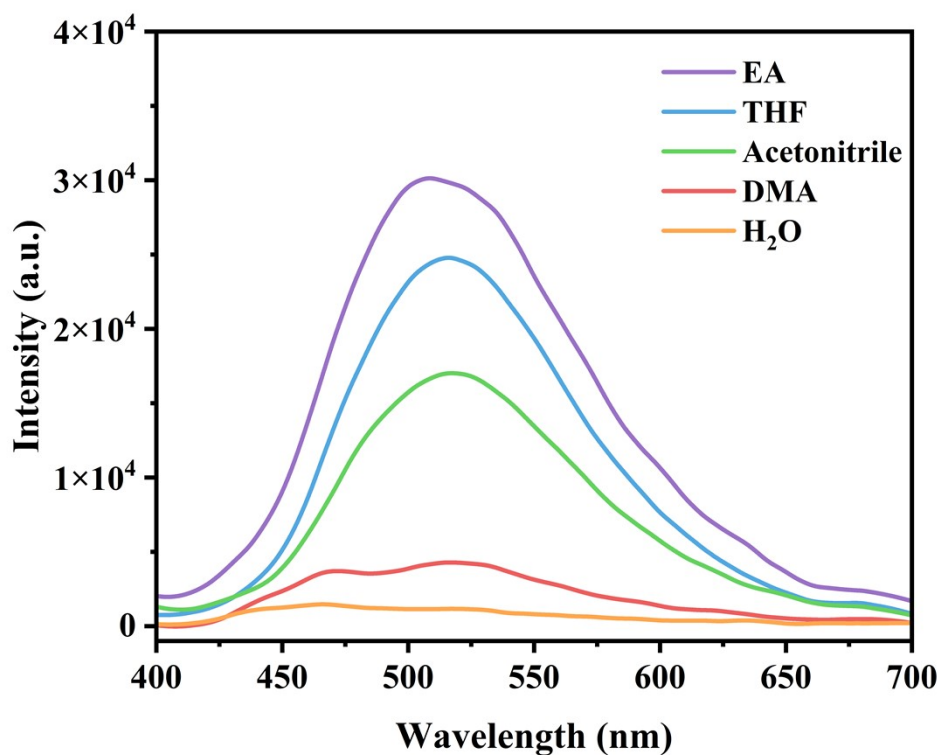


Figure S21. The emission spectra of PATM in different solvents ($\lambda_{\text{ex}}=360$ nm).

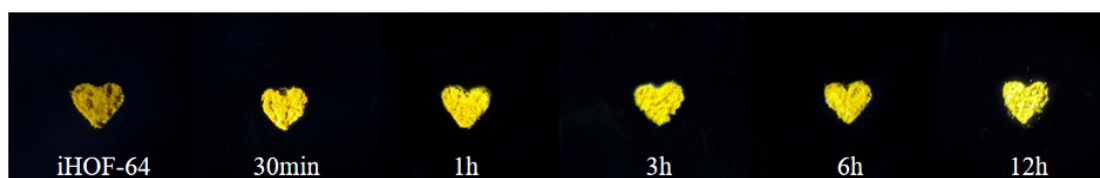


Figure S22. The fluorescence color changes of **iHOF-64** after being immersed in DMA solvent for different times.

Table S2. The intermolecular interactions between **iHOF-64** and **iHOF-65**.

iHOF-64		iHOF-65	
N-H...O	Distance(Å)	N-H...O	Distance(Å)
N2-H2B...O3	2.15	N2-H2B...O2	1.95
N4-H4B...O5	1.97	N4-H4B...O5	2.00
N8-H8B...O1	2.01	N8-H8B...O1	1.93
N9-H9B...O6	1.92	N10-H10B...O4	2.14
N7-H7B...O8 ^{#1}	2.08	N7-H7B...O8 ^{#2}	2.43
N10-H10B...O10 ^{#1}	2.07	N9-H9B...O10 ^{#2}	1.98
N3-H3B...O9 ^{#3}	1.97	N5-H5B...O12 ^{#3}	2.04
N5-H5B...O11 ^{#3}	2.15	N3-H3B...O7 ^{#3}	2.05

Symmetry codes: #1: 2-X, 1-Y, 2-Z; #2: 1-X, 1-Y, -Z; #3: 1-X,1-Y,1-Z

Table S3. Quantum yields (Φ), fluorescence lifetimes (τ), radiative rates (k_r) and non-radiative rates (k_{nr}) of **iHOF-64** and **iHOF-65**. $k_r = \Phi/\tau$; $k_{nr} = (1-\Phi)/\tau$.

iHOF	Φ [%]	τ [ns]	k_r [s^{-1}]	k_{nr} [s^{-1}]
iHOF-64	≈ 0	2.4	0	4.17×10^8
iHOF-65	2.02%	2.46	8.21×10^6	3.98×10^8
PATM	≈ 0	0.57	0	1.75×10^9
H ₄ TPE	72.5%	1.95	3.72×10^8	1.41×10^8

Supplementary Reference.

1. M.-F. Huang, L.-H. Cao, B. Zhou, *Chem. Commun.*, 2024, **60**, 3437-3440.
2. A. K. Rashid, R. B. Yahya, P. S. Wai, *Asian Journal of Chemistry.*, 2014, **26**, 3854-3862.
3. M. Morshedi, M. Thomas, A. Tarzia, C. J. Doonan and N. G. White, *Chem. Sci.*, 2017, **8**, 3019-3025.
4. O. V. Dolomanov, L. J. Bourhis, R. J. Gildea, J. A. K. Howard, H. Puschmann, *J. Appl. Cryst.*, 2009, **42**, 339-341.
5. G. M. Sheldrick, *Acta Cryst.*, 2015, **A71**, 3-8.
6. G. M. Sheldrick, *Acta Cryst.*, 2015, **C71**, 3-8.